# A Hybrid Phase Flow Method for solving Liouville Equation in Bounded Domain*

Hao Wu† and Xu Yang‡

September 11, 2010

**Abstract**

The phase flow method was originally introduced in [28] which can efficiently solve autonomous ordinary differential equations. In [13], the method was generalized to solve Hamiltonian system where the Hamiltonian function was discontinuous. However, both these methods require phase flow map constructed on an *invariant* manifold. This can increase computational cost when the invariant domain is big or unbounded.

Following the idea of [13], we propose a hybrid phase flow method for solving Liouville equation in bounded domain, which is smaller than the invariant manifold of phase flow map. By using some proper boundary conditions, this method can help solve the problem where the invariant manifold of phase flow map determined by Liouville equation is unbounded. We verify numerical accuracy and efficiency by several examples of the semiclassical limit of Schrödinger equation. Analysis of numerical stability and convergence is given for the semiclassical limit equation with inflow boundary condition.

**Key words:** phase flow method, Liouville equation, high frequency wave, particle method, Hamiltonian system

## 1 Introduction

In recent years, computation of high frequency waves has received lots of attention because of its importance in seismology, electromagnetic waves and quantum mechanics. Efficient numerical methods have been developed with the help of WKB analysis [15, 1, 4], level set framework [11, 9, 2]

*This work was partially supported by NSFC Projects 11071139 and NSFC Projects 10971115.

†Department of Mathematical Sciences, Tsinghua University, Beijing, 10084, China (hwu@tsinghua.edu.cn)

‡Program in Applied and Computational Mathematics, Princeton University, NJ 08544, USA (xuyang@math.princeton.edu)

and Gaussian beam methods [19, 21, 24, 14]. Reviews of these methods were given in [3, 22]. In applying these methods, one has to deal with the following Liouville equation

$$f_t + \nabla_{\boldsymbol{\xi}} H \cdot \nabla_{\boldsymbol{x}} f - \nabla_{\boldsymbol{x}} H \cdot \nabla_{\boldsymbol{\xi}} f = 0,\ t > 0,\ \boldsymbol{x}, \boldsymbol{\xi} \in \mathbb{R}^d, \tag{1}$$

which serves as the semiclassical limit of the Schrödinger equation or wave equation ([3, 7, 18]).

In (1) $f(t, \boldsymbol{x}, \boldsymbol{\xi}) \geq 0$ is the probability density function at time $t$, position $\boldsymbol{x}$ and velocity $\boldsymbol{\xi}$. The Hamiltonian function $H = H(\boldsymbol{x}, \boldsymbol{\xi}) : \mathbb{R}^{2d} \to \mathbb{R}$ has either the form

$$H = \frac{|\boldsymbol{\xi}|^2}{2} + V(\boldsymbol{x}), \tag{2}$$

for Schrödinger equation where $V(\boldsymbol{x})$ is the potential, or

$$H = c(\boldsymbol{x})\,|\boldsymbol{\xi}|\,, \tag{3}$$

for wave equation where $c(\boldsymbol{x}) > 0$ is the local wave speed.

The domain for (1) is taken as

$$M = \left\{ (\boldsymbol{x}, \boldsymbol{\xi}) \in \mathbb{R}^{2d} \mid \boldsymbol{x} \in X,\ H_{\min} \leq H(\boldsymbol{x}, \boldsymbol{\xi}) \leq H_{\max} \right\},$$

where $X \subset \mathbb{R}^d$ is bounded and closed in physical space.

Particle method for (1) is based on solving the Hamiltonian system,

$$\frac{\mathrm{d}\boldsymbol{x}}{\mathrm{d}t} = -\nabla_{\boldsymbol{\xi}} H, \tag{4}$$

$$\frac{\mathrm{d}\boldsymbol{\xi}}{\mathrm{d}t} = \nabla_{\boldsymbol{x}} H, \tag{5}$$

which are actually the equations of bicharacteristics of (1) after reversing time $t \to -t$.

In [28], Ying and Candés proposed a novel phase flow method which computed (4)-(5) efficiently for multiple initial conditions. This method was later generalized to solve (4)-(5) in heterogeneous media in [13]. The key idea of phase flow method is to construct the flow map $h_t : \mathbb{R}^{2d} \to \mathbb{R}^{2d}$ by using its group property and doing numerical interpolation efficiently on an *invariant* manifold $M$. $h_t$ is defined by $h_t(\boldsymbol{x}_0, \boldsymbol{\xi}_0) = (\boldsymbol{x}(t), \boldsymbol{\xi}(t))$ and invariant manifold $M$ means $h_t(M) \subset M$.

However, since the Liouville equation (1) is considered in a bounded domain, it can not always satisfy the constraint of invariance $h_t(M) \subset M$. On the other hand, even if we consider (1) in the whole phase space, the constraint of $M$ being invariant can increase computational cost when the size of $M$ is large. One can meet such cases in many common Hamiltonian systems. For example, if we consider the Hamiltonian in classic mechanics

$H = \frac{1}{2}|\boldsymbol{\xi}|^2 + V(\boldsymbol{x})$ and take the potential $V(\boldsymbol{x}) = 0$, the invariant domain of the phase flow (4)-(5) is $\{(\boldsymbol{x}, \boldsymbol{\xi}) | \boldsymbol{x} \in \mathbb{R}^d,\ \boldsymbol{\xi} \in \boldsymbol{\Xi}\}$ which is unbounded.

Following the idea of [13], we develop a hybrid phase flow method to solve (1) in a bounded domain. This also offers a way to reduce computational cost in the traditional phase flow method when the invariant manifold of (4)-(5) is unbounded by using some proper boundary conditions.

The general inflow boundary condition for (1) is given by

$$f(t, \boldsymbol{x}, \boldsymbol{\xi})|_{x \in \partial X, \nabla_{\boldsymbol{\xi}} H \cdot \boldsymbol{n} > 0} = g(t, \boldsymbol{x}, \boldsymbol{\xi}), \tag{6}$$

where $\boldsymbol{n}$ denotes the inward normal direction of the boundary $\partial X$, and the initial condition is

$$f(0, \boldsymbol{x}_0, \boldsymbol{\xi}_0) = f_0(\boldsymbol{x}_0, \boldsymbol{\xi}_0). \tag{7}$$

Since the Hamiltonian functions that we mostly concern are in the form of (2) and (3), we rewrite the inflow boundary condition for convenience

$$f(t, \boldsymbol{x}, \boldsymbol{\xi})|_{x \in \partial X,\ \boldsymbol{\xi} \cdot \boldsymbol{n} > 0} = g(t, \boldsymbol{x}, \boldsymbol{\xi}). \tag{8}$$

We consider (4)-(5) with initial conditions

$$\boldsymbol{x}(0) = \boldsymbol{x}_0,\ \boldsymbol{\xi}(0) = \boldsymbol{\xi}_0,$$

and define the phase flow solution $h_T(\boldsymbol{x}_0, \boldsymbol{\xi}_0)$ as follows (for $T > 0$),

Case 1. $\boldsymbol{x}(t; \boldsymbol{x}_0, \boldsymbol{\xi}_0) \in \mathring{X},\ \forall t \in [0, T]$. The particle stays inside the physical space $X$. The phase flow solution is given by

$$h_T(\boldsymbol{x}_0, \boldsymbol{\xi}_0) = (\boldsymbol{x}(T; \boldsymbol{x}_0, \boldsymbol{\xi}_0), \boldsymbol{\xi}(T; \boldsymbol{x}_0, \boldsymbol{\xi}_0)). \tag{9}$$

Case 2. $\exists t \in [0, T],\ \boldsymbol{x}(t; \boldsymbol{x}_0, \boldsymbol{\xi}_0) \in \partial X$. The particle trajectory collides with the boundary $\partial X$. The phase flow solution is given by

$$h_T(\boldsymbol{x}_0, \boldsymbol{\xi}_0) = (\boldsymbol{x}(t'; \boldsymbol{x}_0, \boldsymbol{\xi}_0), \boldsymbol{\xi}(t'; \boldsymbol{x}_0, \boldsymbol{\xi}_0)), \tag{10}$$

where the $t' = t'(\boldsymbol{x}_0, \boldsymbol{\xi}_0)$ is the first arrival time

$$t' = \inf\{t \in [0, T] \big| \boldsymbol{x}(t; \boldsymbol{x}_0, \boldsymbol{\xi}_0) \in \partial X\}. \tag{11}$$

The solution $f(T, \boldsymbol{x}, \boldsymbol{\xi})$ to (1) is given by method of characteristics,

$$f(T, \boldsymbol{x}, \boldsymbol{\xi}) = \begin{cases} f_0(h_T(\boldsymbol{x}, \boldsymbol{\xi})), & \text{particle moves inside } X, \\ g(h_T(T - t'(\boldsymbol{x}, \boldsymbol{\xi}), \boldsymbol{x}, \boldsymbol{\xi})), & \text{particle coincides with } \partial X. \end{cases} \tag{12}$$

A diagram is given in Figure 1 to illustrate how the initial and boundary conditions are used to determine the solution $f(T, \boldsymbol{x}, \boldsymbol{\xi})$.

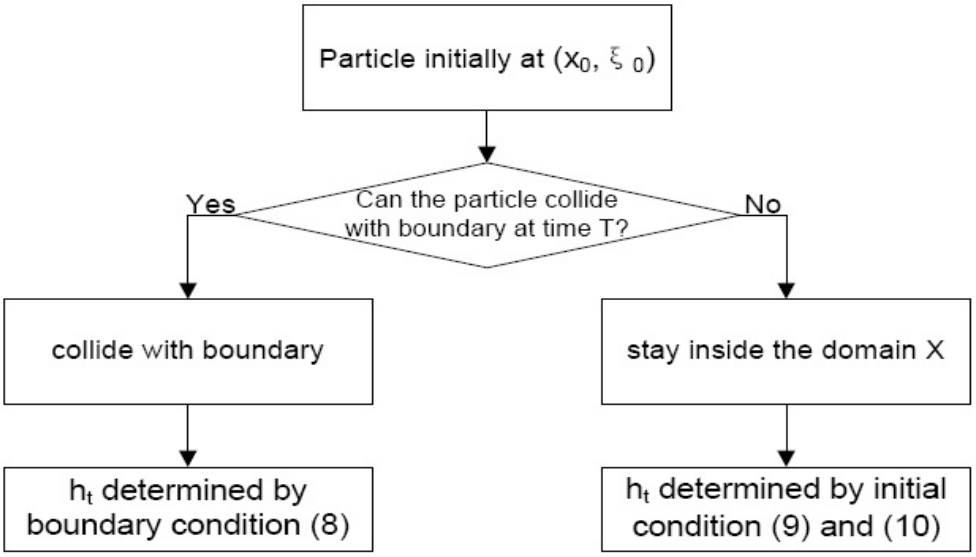


Figure 1: Diagram of how initial and boundary conditions are used to determine the solution at time $T$.

**Remark 1.1** *The algorithm can be also applied for reflection boundary condition*

$$f(t,\boldsymbol{x},\boldsymbol{\xi})|_{x\in\partial X,\nabla_{\boldsymbol{\xi}}H\cdot\boldsymbol{n}>0}=f(t,\boldsymbol{x},\boldsymbol{\xi}^*),$$

*where* $\boldsymbol{\xi}^*$ *satisfies*

$$\nabla_{\boldsymbol{\xi}}H(\boldsymbol{x},\boldsymbol{\xi}^*)=\nabla_{\boldsymbol{\xi}}H(\boldsymbol{x},\boldsymbol{\xi})-2\left(\nabla_{\boldsymbol{\xi}}H(\boldsymbol{x},\boldsymbol{\xi})\cdot\boldsymbol{n}\right)\boldsymbol{n}.$$

*For Hamiltonian functions* (2) *and* (3)*, the reflection boundary condition can be simplified as*

$$f(t,\boldsymbol{x},\boldsymbol{\xi})|_{x\in\partial X,\boldsymbol{\xi}\cdot\boldsymbol{n}>0}=f(t,\boldsymbol{x},\boldsymbol{\xi}-2\left(\boldsymbol{\xi}\cdot\boldsymbol{n}\right)\boldsymbol{n}).$$

*The solution* $f(T,\boldsymbol{x},\boldsymbol{\xi})$ *is given by*

$$f(T,\boldsymbol{x},\boldsymbol{\xi})=f_0(h_T(\boldsymbol{x},\boldsymbol{\xi})),$$

*where* $h_T$ *is constructed using the algorithm in [13] by considering boundary as interface with total reflection.*

The rest of paper is organized as follows. In Section 2, we introduce the hybrid phase flow method to solve Liouville equation in bounded domain. The analysis of numerical stability and convergency is discussed in Section 3. Along with the algorithm developed in [13], this method is very useful in computing the high frequency waves which we discuss in Section 4. In Section 5, we make some conclusive remarks.

## 2 The hybrid phase flow method

In this section we introduce how to construct $h_t$ on the bounded domain $M$ at time $T$. We select a small time step $\tau > 0$ and an integer constant $K \geq 1$ so that $B = (T/\tau)^{1/K}$ is an integer power of 2. The general procedure is described as follows:

1. Discretization. Start with a uniform or quasi-uniform grid $M_h$ of $M$.
2. Initialization. Compute an approximation of $h_\tau$.
   (a) For $(\boldsymbol{x}_0, \boldsymbol{\xi}_0)$ in $M_h$, $h_\tau(\boldsymbol{x}_0, \boldsymbol{\xi}_0)$ is computed by numerical Hamiltonian solver $\Theta_\tau$ on bounded domain. $\Theta_\tau$ is described in details in Section 2.1.
   (b) For $(\boldsymbol{x}_0, \boldsymbol{\xi}_0)$ not in $M_h$, $h_\tau$ is given via either a local interpolation $\mathcal{I}$ (for regular particles) or numerical Hamiltonian solver $\Theta_\tau$ (for special particles).
3. Loop. Construct $h_{B^{k+1}\tau}$ from $h_{B^k\tau}$, loop for $b = 1, \cdots, B-1$,
   (a) For $(\boldsymbol{x}_0, \boldsymbol{\xi}_0)$ in $M_h$,
   $$h_{(b+1)\cdot B^k\tau}(\boldsymbol{x}_0, \boldsymbol{\xi}_0) = h_{B^k\tau}(h_{b\cdot B^k\tau}(\boldsymbol{x}_0, \boldsymbol{\xi}_0)).$$
   (b) For $(\boldsymbol{x}_0, \boldsymbol{\xi}_0)$ not in $M_h$, one needs to use the local interpolation $\mathcal{I}$ (for regular particles) or the numerical Hamiltonian solver $\Theta_\tau$ (for special particles) to construct $h_{B^{k+1}\tau}$.

The detailed implementation is given in Section 2.2.

### 2.1 A numerical Hamiltonian solver for bounded domain

In this subsection, we design the numerical Hamiltonian solver

$$\begin{array}{rccc} \Theta_{\Delta t}: & M \subset \mathbb{R}^{2d} & \rightarrow & M \subset \mathbb{R}^{2d} \\ & (\boldsymbol{x}^n, \boldsymbol{\xi}^n) & \rightarrow & (\boldsymbol{x}^{n+1}, \boldsymbol{\xi}^{n+1}) \end{array}$$

for the Hamiltonian system (4)-(5). For convenience, we denote $\Gamma_{\Delta t}(\boldsymbol{x}, \boldsymbol{\xi}) : \mathbb{R}^{2d} \rightarrow \mathbb{R}^{2d}$ as the one-step standard sympletic numerical solvers given in [6, 16], for example, the Verlet scheme.

1. Estimate the position and velocity of particle $(\boldsymbol{x}^*, \boldsymbol{\xi}^*) = \Gamma_{\Delta t}(\boldsymbol{x}^n, \boldsymbol{\xi}^n)$.
2. If $\boldsymbol{x}^* \in \mathring{X}$, *i.e.* the particle moves inside domain $X$ during $[t^n, t^{n+1}]$, we set $(\boldsymbol{x}^{n+1}, \boldsymbol{\xi}^{n+1}) = (\boldsymbol{x}^*, \boldsymbol{\xi}^*)$.
3. Otherwise,

(a) Approximate the first arrival time $\Delta t^\star = \frac{d(\boldsymbol{x}^n)}{d(\boldsymbol{x}^*)+d(\boldsymbol{x}^n)}\Delta t$ where $d(\boldsymbol{x})$ is the distance to the boundary $\partial X$.

(b) Approximate the first arrival position and velocity $(\boldsymbol{x}^\star, \boldsymbol{\xi}^\star) = \Gamma_{\Delta t^\star}(\boldsymbol{x}, \boldsymbol{\xi})$.

(c) Set $(\boldsymbol{x}^{n+1}, \boldsymbol{\xi}^{n+1}) = (\boldsymbol{x}^\star, \boldsymbol{\xi}^\star)$.

**Remark 2.1** *In Section 3, the numerical Hamiltonian solver $\Theta_\tau$ will be proved to converge at second order. The numerical accuracy can be improved by using higher order sympletic numerical solvers and approximating the first arrival time more accurately.*

**Remark 2.2** *We use sympletic numerical integrators in the implementation of algorithm. One can also use nonsympletic ones, for example Runge-Kutta schemes, but it gets more involved in the part of analysis.*

## 2.2 The detailed implementation

Now we are ready to describe hybrid phase flow method for bounded domain in details. The important part is to identify different types of particles. We first introduce several symbols.

**Symbol 1** *$N_i^{(k)} = (\boldsymbol{x}_i^{(k)}, \boldsymbol{\xi}_i^{(k)}) \in M$ is the position and velocity of the particle after $k$ iterations, which initially starts at $N_i^{(0)} = (\boldsymbol{x}_i^{(0)}, \boldsymbol{\xi}_i^{(0)})$. Note that the initial mesh is $M_h = \{N_i^{(0)},\ \forall i\}$.*

**Symbol 2** *Denote $G_j$ as the mesh cells, and $\mathcal{N}(G_j) = \{N_{j_1}^{(0)}, \cdots, N_{j_l}^{(0)}\}$ as the set of all vertices (mesh points) of $G_j$. Define $\mathcal{G}(\boldsymbol{x}, \boldsymbol{\xi}) = j$, if $(\boldsymbol{x}, \boldsymbol{\xi}) \in G_j$.*

**Symbol 3** *Denote $\mathcal{S}(N_i^{(0)})$ as the current status of the particle initially starting at $N_i^{(0)}$,*

$$\mathcal{S}(N_i^{(0)}) = \begin{cases} 0, & \text{if particle has coincided with boundary } \partial X, \\ 1, & \text{otherwise.} \end{cases}$$

**Symbol 4** *Define $\mathcal{I}_1$ as the evolutional interpolation function, and*

$$(\boldsymbol{y}^*, \boldsymbol{\eta}^*) = \mathcal{I}_1\left((\boldsymbol{x}^1, \boldsymbol{\xi}^1), \cdots, (\boldsymbol{x}^l, \boldsymbol{\xi}^l), (\boldsymbol{y}^1, \boldsymbol{\eta}^1), \cdots, (\boldsymbol{y}^l, \boldsymbol{\eta}^l); (\boldsymbol{x}^*, \boldsymbol{\xi}^*)\right),$$

*where $\mathcal{I}_1$ interpolates the values $(\boldsymbol{y}^i, \boldsymbol{\eta}^i) \in M (i = 1, \cdots, l)$ at points $(\boldsymbol{x}^i, \boldsymbol{\xi}^i) \in M$, and gives the value $(\boldsymbol{y}^*, \boldsymbol{\eta}^*) \in M$ for $(\boldsymbol{x}^*, \boldsymbol{\xi}^*) \in M$, .*

**Symbol 5** *Define $\mathcal{I}_2$ as the first arrival interpolation function, and*

$$(t^*, \boldsymbol{y}^*, \boldsymbol{\eta}^*) = \mathcal{I}_2\left((\boldsymbol{x}^1, \boldsymbol{\xi}^1), \cdots, (\boldsymbol{x}^l, \boldsymbol{\xi}^l), (t^1, \boldsymbol{y}^1, \boldsymbol{\eta}^1), \cdots, (t^l, \boldsymbol{y}^l, \boldsymbol{\eta}^l); (\boldsymbol{x}^*, \boldsymbol{\xi}^*)\right),$$

*where* $(\boldsymbol{y}^i, \boldsymbol{\eta}^i) \in M$ *and* $\boldsymbol{y}^i \in \partial X$. $\mathcal{I}_2$ *interpolates through points* $(\boldsymbol{x}^i, \boldsymbol{\xi}^i) \in M$, *the values* $t^i$, $\boldsymbol{y}^i$ *and* $\boldsymbol{\eta}^i$ *denoting the first arrival time, position and velocity, and gives the value* $(t^*, \boldsymbol{y}^*, \boldsymbol{\eta}^*)$ *for* $(\boldsymbol{x}^*, \boldsymbol{\xi}^*) \in M$ *where* $(\boldsymbol{y}^*, \boldsymbol{\eta}^*) \in M$ *and* $\boldsymbol{y}^* \in \partial X$.

**Symbol 6** *Let* $t' = t'(\boldsymbol{x}, \boldsymbol{\xi}) : M \to [0, +\infty) \cup \{-1\}$ *be the first arrival time when the particle initially at* $(\boldsymbol{x}, \boldsymbol{\xi})$ *collides with the boundary* $\partial X$. *If the particle never collides with the boundary* $\partial X$, *it will be set to be* $-1$.

The detailed implementation of the algorithm:

1. Discretization. Assume we start with a uniform or quasi-uniform mesh $M_h = \{N_i^{(0)} |\ i = 1, \cdots, I\}$, then $G_j$ and $\mathcal{N}(G_j)$ $(j = 1, \cdots, J)$ are well defined. The stopping time is $t = T$. The time $\tau$ and number of iterations $K \geq 1$ is selected to satisfy $B = (T/\tau)^{1/K}$ is an integer power of 2.

2. Initialization. Set $k = 1$. For $i = 1, \cdots, I$
$$N_i^{(1)} = \Theta_\tau(N_i^{(0)}).$$
Since the numerical Hamiltonian solver $\Theta_\tau$ can automatically check whether the particle trajectory collides with boundary during $[0, \tau]$, we set
$$\mathcal{S}(N_i^{(0)}) = 0,\ t'(N_i^{(0)}) = \Delta t^\star,$$
for the particles that collide with boundary, and
$$\mathcal{S}(N_i^{(0)}) = 1,\ t'(N_i^{(0)}) = -1,$$
for the particles that stay inside domain $X$.

3. Loop at the $k$th iteration. For $i = 1, \cdots, I$
$$N_i^{(k+1)} = N_i^{(k)}.$$
The following is looped for $b = 1, \cdots, B - 1$.

   - For those particles satisfying $\mathcal{S}(N_i^{(0)}) = 1$, there is $j = \mathcal{G}(N_i^{(k+1)})$ such that $N_i^{(k+1)} \in G_j$. We check the status value of all vertices $N_m^{(0)} \in \mathcal{N}(G_j),\ m \in \{j_1, j_2, \cdots, j_l\}$ to update $N_i^{(k+1)}$.
     (a) If $\mathcal{S}(N_m^{(0)}) = 0,\ \forall m \in \{j_1, j_2, \cdots, j_l\}$, $N_i^{(k+1)}$ is called boundary particle, and we compute the first arrival time $t'(N_i^{(0)})$ and the value of $N_i^{(k+1)}$ by local interpolation,
$$\begin{aligned}\left(t'(N_i^{(0)}), N_i^{(k+1)}\right) \ &= \ \mathcal{I}_2\Big(N_{j1}^{(0)}, \cdots, N_{jl}^{(0)}, \left(t'(N_{j1}^{(0)}), N_{j1}^{(k)}\right), \\ &\qquad \cdots, \left(t'(N_{jl}^{(0)}), N_{jl}^{(k)}\right); N_i^{(k+1)}\Big).\end{aligned}$$

The particle status value is updated to be

$$\mathcal{S}(N_i^{(0)}) = 0.$$

(b) If $\mathcal{S}(N_m^{(0)}) = 1,\ \forall m \in \{j_1, j_2, \cdots, j_l\}$, $N_i^{(k+1)}$ is called standard particle, and we define the new value of $N_i^{(k+1)}$ by the local interpolation,

$$N_i^{(k+1)} = \mathcal{I}_1\left(N_{j1}^{(0)}, \cdots, N_{jl}^{(0)}, N_{j1}^{(k)}, \cdots, N_{jl}^{(k)}; N_i^{(k+1)}\right).$$

The last two types of particles are named *regular* particles.

(c) Otherwise if $\mathcal{S}(N_m^{(0)}) = 0$ for only some $m \in \{j_1, j_2, \cdots, j_l\}$, $N_i^{(k+1)}$ is called special particle, and we decide the new value of $N_i^{(k+1)}$ by the numerical Hamiltonian solver $\Theta_\tau$: update the value of $N_i^{(k+1)}$ for $B^k$ times by

$$N_i^{(k+1)} = \Theta_\tau(N_i^{(k+1)}).$$

If the particle collides with the boundary at some step $k'$, the first arrival time is

$$t'(N_i^{(0)}) = (b \cdot B^k + k' - 1)\tau + \Delta t^\star.$$

The particle status value is updated to be

$$\mathcal{S}(N_i^{(0)}) = 0.$$

- For particle satisfies $\mathcal{S}(N_i^{(0)}) = 0$, meaning that the particle has already collided with boundary, its value will not change any more.

4. If $k + 1 = K$, stop. Otherwise we let $k = k + 1$ and go to step 3.

By the above procedure, we obtain the position and velocity $N_i^{(K)}$ of the particle at time $T = B^K\tau$, which initially starts at $N_i^{(0)}(i = 1, \cdots, I)$. For these particles colliding with boundary, we have an approximation of the first arrival time $t'(N_i^{(0)})$.

**Remark 2.3** *Along with the method in [13], this algorithm can be easily generalized to the interface problem where the Hamiltonian function is discontinuous. This will be studied later in the numerical examples.*

**Remark 2.4** *Similar to the discussions in [13], the number of special particles is $O(N^{2d-1})$ on a 2d-dimensional phase space lattice $M_h$ with $N$ particles in each direction. This will be numerically verified in Section 4. So the total computational complexity for the Hybrid phase flow method is $O(N^{2d-1}L + N^{2d}L^{1/s})$ with $L = B^K$.*

# 3 Stability and convergence

In this section we analyze stability and convergence of the hybrid phase flow method. For the purpose of simplicity and clarity, we investigate the one-dimensional problem in classical mechanics where the Hamiltonian $H : \mathbb{R}^2 \to \mathbb{R}$ is given by

$$H(x, \xi) = \frac{1}{2}\xi^2 + V(x),$$

where the potential $V(x) \in C^\infty(X)$. The bounded and closed domain $X \subset \mathbb{R}$ is taken as $X = [-1, 1]$. The force function of Hamiltonian system (4)-(5)

$$F(x, \xi) = (-\xi, V'(x))^T$$

is smooth and has Lipschitz constant $L$ on $X$.

## 3.1 Analysis of the algorithm stability

We first study the stability of the phase flow solution $h_t$ under some reasonable assumptions that all the particles lie in the domain

$$D = \left\{(x, \xi) \in \mathbb{R}^2 \;\middle|\; \left|H(x, \xi) - V(\pm 1)\right| > \epsilon_0\right\}$$

where $\epsilon_0 > 0$ is a small parameter. This removes the physical unstable cases where the particles have zero velocity at the boundaries $x = \pm 1$ but will travel into the domain $M$ under small perturbations.

**Theorem 3.1** *The phase flow solution $h_t$ defined in Section 1 is stable on $D \cap M$, with the estimate*

$$\|h_t(x_1, \xi_1) - h_t(x_2, \xi_2)\| \leq L_1 e^{L_2 t} \|(x_1, \xi_1) - (x_2, \xi_2)\|,$$

*where $L_1$ and $L_2$ are constants.*

**Proof:**(I) If $x(t'; x_i, \xi_i) \in \mathring{X},\ \forall t' \in [0, t], i = 1, 2$, which means both the particles always stay inside $X$, it is easy to have

$$\|h_t(x_1, \xi_1) - h_t(x_2, \xi_2)\| \leq e^{Lt} \|(x_1, \xi_1) - (x_2, \xi_2)\|, \tag{13}$$

by using Gronwall's inequality.

(II) If $\exists t' \in [0, t],\ x(t'; x_i, \xi_i) \in \partial X,\ i = 1, 2$, which means at least one particle trajectory collides with boundary $\partial X$. Without loss of of generality, we can assume that there exists $t_a \in [0, t)$ satisfies,

i. $x(t_a; x_1, \xi_1) \in \partial X$,

ii. $x(t'; x_1, \xi_1) \in \mathring{X},\ \forall t' \in [0, t_a)$,

iii. $x(t';x_2,\xi_2)\in \mathring{X},\ \forall t'\in[0,t_a]$.

By (I) and the closeness of $X$, we have

$$\|h_{t_a}(x_1,\xi_1)-h_{t_a}(x_2,\xi_2)\|\le e^{Lt_a}\|(x_1,\xi_1)-(x_2,\xi_2)\|. \tag{14}$$

Let

$$\begin{aligned} t_b &= t-t_a,\\ (x_3,\xi_3) &= h_{t_a}(x_1,\xi_1),\\ (x_4,\xi_4) &= h_{t_a}(x_2,\xi_2), \end{aligned}$$

then we have

$$\begin{aligned} \|h_t(x_1,\xi_1)-h_t(x_2,\xi_2)\| &= \|h_{t_b}(h_{t_a}(x_1,\xi_1))-h_{t_b}(h_{t_a}(x_2,\xi_2))\|\\ &= \|h_{t_b}(x_3,\xi_3)-h_{t_b}(x_4,\xi_4)\|\\ &= \|(x_3,\xi_3)-h_{t_b}(x_4,\xi_4)\|. \end{aligned} \tag{15}$$

The last equality is due to $x_3\in\partial X$. Without loss of generality we assume $x_3=1$, then the velocity $\xi_3>\sqrt{2\epsilon_0}$ since $(x_3,\xi_3)\in D$. We prove the conclusion by discussing the following two cases.

Case 1. $x(t';x_4,\xi_4)\in\mathring{X},\ \forall t'\in[0,t_b]$. We define a new phase flow solution

$$\widehat{h}_t(x_0,\xi_0)=(\widehat{x}(t;x_0,\xi_0),\widehat{\xi}(t;x_0,\xi_0)),$$

by extending the potential $V$ in (4)-(5) to domain $[-1,\infty]$

$$\widehat{V}(x)=\begin{cases} V(1)+\frac{1}{2}V'(1)\zeta, & x\in[1+\zeta,\infty),\\ -\frac{1}{2\zeta}V'(1)(x-1)^2+V'(1)(x-1)+V(1), & x\in(1,1+\zeta),\\ V(x), & x\in[-1,1], \end{cases}$$

where $\zeta=\min(\frac{1}{2}\epsilon_0,\frac{\epsilon_0}{|V'(1)|})$. It is easy to verify that $\widehat{V}\in C^1([-1,\infty))$ and $\widehat{F}$ has Lipschitz constant $L'=\max(L,\frac{|V'(1)|}{\zeta})$ on $[-1,\infty)$. Then we have

$$\left\|\widehat{h}_t(x_3,\xi_3)-\widehat{h}_t(x_4,\xi_4)\right\|\le e^{L't_b}\|(x_3,\xi_3)-(x_4,\xi_4)\|.$$

Since $\xi_3>\sqrt{2\epsilon_0}$ and $\left|\frac{1}{2}V'(1)\zeta\right|<\frac{1}{2}\epsilon_0$, the velocity $\widehat{\xi}(t';x_3,\xi_3)>0,\ \forall t'\in[0,t_b]$. This induces $\widehat{x}(t_b;x_3,\xi_3)>x_3>\widehat{x}(t_b;x_4,\xi_4)=x(t_b;x_4,\xi_4)$ and

$$\begin{aligned} |x_3-x(t_b;x_4,\xi_4)| &< |\widehat{x}(t_b;x_3,\xi_3)-\widehat{x}(t_b;x_4,\xi_4)|,\\ |x_3-\widehat{x}(t_b;x_3,\xi_3)| &< |\widehat{x}(t_b;x_3,\xi_3)-\widehat{x}(t_b;x_4,\xi_4)|. \end{aligned} \tag{16}$$

On the other hand, we have

$$\begin{aligned} &|\xi_3-\xi(t_b;x_4,\xi_4)|\\ \le\ &\left|\widehat{\xi}(t_b;x_3,\xi_3)-\widehat{\xi}(t_b;x_4,\xi_4)\right|+\left|\xi_3-\widehat{\xi}(t_b;x_3,\xi_3)\right|\\ \le\ &\left|\widehat{\xi}(t_b;x_3,\xi_3)-\widehat{\xi}(t_b;x_4,\xi_4)\right|+L''\,|x_3-\widehat{x}(t_b;x_3,\xi_3)| \qquad (17)\\ <\ &\left|\widehat{\xi}(t_b;x_3,\xi_3)-\widehat{\xi}(t_b;x_4,\xi_4)\right|+L''\,|\widehat{x}(t_b;x_3,\xi_3)-\widehat{x}(t_b;x_4,\xi_4)|. \qquad (18) \end{aligned}$$

The inequality (17) holds based on the observation that

$$\xi(x) = \sqrt{\xi_3^2 + 2(V(x_3) - \widehat{V}(x))}$$

has the Lipschitz constant $L'' = \max(L, \frac{|\widehat{V}'(x)|}{2\epsilon_0})$ on $[-1, \infty)$.

(14)-(16) and (18) imply

$$\begin{aligned} \|h_t(x_1,\xi_1) - h_t(x_2,\xi_2)\| &= \|(x_3,\xi_3) - h_{t_b}(x_4,\xi_4)\| \\ &\leq (L''+1)\left\|\widehat{h}_t(x_3,\xi_3) - \widehat{h}_t(x_4,\xi_4)\right\| \\ &\leq L_1 e^{L_2 t_b}\|(x_3,\xi_3) - (x_4,\xi_4)\| \\ &\leq L_1 e^{L_2 t}\|(x_1,\xi_1) - (x_2,\xi_2)\|. \end{aligned} \tag{19}$$

where $L_1 = L'' + 1$ and $L_2 = L'$ are constants.
Case 2. $\exists t' \in [0, t_b],\ x(t'; x_4, \xi_4) \in \partial X$. Let $t_c \leq t_b$ be the first arrival time. It is easy to see that

$$\begin{aligned} \|h_T(x_1,\xi_1) - h_T(x_2,\xi_2)\| &= \|(x_3,\xi_3) - h_{t_b}(x_4,\xi_4)\| \\ &= \|(x_3,\xi_3) - h_{t_c}(x_4,\xi_4)\| \\ &\leq L_1 e^{L_2 t_c}\|(x_3,\xi_3) - (x_4,\xi_4)\| \\ &\leq L_1 e^{L_2 t}\|(x_1,\xi_1) - (x_2,\xi_2)\|. \end{aligned} \tag{20}$$

(13), (19) and (20) prove the theorem. ■

### 3.2 Convergence Analysis of the Algorithm

In this subsection we prove the convergence of the hybrid phase flow method.

**Theorem 3.2** *The numerical Hamiltonian solver $\Theta_\tau$ described in Section 2.1 converges with a second order accuracy on $D \cap M$.*

**Proof:** Since the one-step standard symplectic numerical solver $\Gamma_\Delta$ converges at second order when the particle stays inside the configuration space domain $X$, we only need to consider the situation when the particle is very near the boundary, *i.e.* for small enough $\Delta t$,

$$\|\Theta_{\Delta t}(x_0,\xi_0) - h_{\Delta t}(x_0,\xi_0)\| \leq C_a \Delta t^2, \tag{21}$$

where $C_a$ is a positive constant, and the particle trajectory collides with boundary $\partial X$ in the short time $\Delta t$.

Let $\Delta t^*$ and $\Delta t^\star$ be the exact arrival time and the estimated arrival time respectively, and $(x_1, \xi_1) = h_{\Delta t^*}(x_0, \xi_0)$ be the position and velocity when the particle collides with boundary $\partial X$. We rewrite sympletic numerical solver $\Gamma_{\Delta t}$ as

$$\Gamma_{\Delta t}(x,\xi) = (x_\Gamma(\Delta t; x, \xi), \xi_\Gamma(\Delta t; x, \xi)).$$

Since $V(x) \in C^\infty(X)$, one can write the sympletic numerical solver as

$$\begin{aligned} x_\Gamma(\Delta t; x, \xi) &= x + v_{11}(x,\xi)\Delta t + v_{21}(x,\xi)\Delta t^2 + O(\Delta t^3), \\ \xi_\Gamma(\Delta t; x, \xi) &= \xi + v_{12}(x,\xi)\Delta t + v_{22}(x,\xi)\Delta t^2 + O(\Delta t^3), \end{aligned}$$

where

$$\|(v_{i1}, v_{i2})\| \le C_i, \quad i = 1, 2.$$

By the approximation formula

$$\begin{aligned} \Delta t^\star &= \frac{x_1 - x_0}{x_\Gamma(\Delta t; x_0, \xi_0) - x_0}\Delta t \\ &= \frac{x_1 - x_0}{v_{11} + v_{21}\Delta t} + O(\Delta t^2), \end{aligned}$$

therefore

$$\begin{aligned} x_\Gamma(\Delta t^\star; x_0, \xi_0) - x_1 &= x_0 + v_{11}\Delta t^\star + v_{21}\Delta t^{\star 2} - x_1 + O(\Delta t^{\star 3}) \\ &= \frac{v_{21}\Delta t(x_0 - x_1)}{v_{11} + v_{21}\Delta t} + v_{21}\Delta t^{\star 2} + O(\Delta t^{\star 3}). \end{aligned}$$

Furthermore

$$\begin{aligned} |x_0 - x_1| &\le |x_0 - x_\Gamma(\Delta t; x_0, \xi_0)| \\ &\le |v_{11}|\,\Delta t + |v_{21}|\,\Delta t^2, \end{aligned}$$

which implies that

$$|x_\Gamma(\Delta t^\star; x_0, \xi_0) - x_1| \le D_1 \Delta t^2,$$

for $\Delta t > 0$ small enough.

Since the numerical solver $\Gamma_\Delta$ is sympletic preserving, we have

$$V(x_\Gamma(\Delta t^\star; x_0, \xi_0)) + \frac{1}{2}\xi_\Gamma^2(\Delta t^\star; x_0, \xi_0) = V(x_1) + \frac{1}{2}\xi_1^2,$$

which gives

$$\begin{aligned} |\xi_\Gamma(\Delta t^\star; x_0, \xi_0) - \xi_1| &\le \frac{2\,|V(x_\Gamma(\Delta t^\star; x_0, \xi_0)) - V(x_1)|}{|\xi_\Gamma(\Delta t^\star; x_0, \xi_0) + \xi_1|} \\ &\le \frac{2D_2\,|x_\Gamma(\Delta t^\star; x_0, \xi_0) - x_1|}{2\sqrt{\epsilon_0}} \\ &\le \frac{D_1 D_2}{\sqrt{\epsilon_0}}\Delta t^2 = D_3 \Delta t^2. \end{aligned}$$

The inequality is based on that $V(x)$ is Lipschitz continuous on $X$ and $(x_0, \xi_0) \in D \cap M$. Taking $C_a = D_1 + D_3$ proves (21).

For any fixed time $T$, we choose the time step $\Delta t$ and the iteration time $N$ such that $N\Delta t = T$. If the particle initially at $(x_0, \xi_0)$ does not collide with boundary $\partial X$,

$$\|\Theta_{N\Delta t}(x_0,\xi_0) - h_T(x_0,\xi_0)\| = \|\Gamma_{N\Delta t}(x_0,\xi_0) - h_T(x_0,\xi_0)\| \le C_b\Delta t^2,$$

where $C_b$ is a constant independent of $T$. For the particle initially at $(x_0, \xi_0)$ collides with boundary $\partial X$, we denote $T_1$ as the colliding time. We choose $t_1 \ge 0$ and an integer $N_1$ such that

$$T_1 = N_1\Delta t + t_1, \text{ and } 0 \le t_1 < \Delta t.$$

Then we have

$$\begin{aligned}
& \|\Theta_{N\Delta t}(x_0,\xi_0) - h_T(x_0,\xi_0)\| \\
= \;& \|\Theta_{t'}(\Gamma_{N_1\Delta t}(x_0,\xi_0)) - h_{t'}(h_{N_1\Delta t}(x_0,\xi_0))\| \\
\le \;& \|\Theta_{t'}(h_{N_1\Delta t}(x_0,\xi_0)) - h_{t'}(h_{N_1\Delta t}(x_0,\xi_0))\| \\
& \qquad + \|\Theta_{t'}(\Gamma_{N_1\Delta t}(x_0,\xi_0)) - \Theta_{t'}(h_{N_1\Delta t}(x_0,\xi_0))\| \\
\le \;& C_a\Delta t^2 + L_1 e^{L_2 t'}\, \|\Gamma_{N_1\Delta t}(x_0,\xi_0) - h_{N_1\Delta t}(x_0,\xi_0))\| \\
\le \;& C_a\Delta t^2 + L_1 e^{L_2 t'} C_b\Delta t^2
\end{aligned}$$

By taking

$$C_0 = \max\left(C_b, C_a + L_1 e^{L_2 t'} C_b\right),$$

we prove the theorem.■

The idea of the proofs for the next lemma and theorem mostly follows those in [28] except with more careful discussions on the cases of boundary particles and special particles.

**Lemma 3.3** *For any multi-index $\gamma$ with $|\gamma| = s \ge 2$, one has*

$$\begin{aligned}
&|\partial^\gamma h_t(x_0,\xi_0)| \le C_s^1 e^{(2s-1)LT}\cdot t, \quad \forall (x_0,\xi_0) \in M_a, \\
&|\partial^\gamma h_t(x_0,\xi_0)| \le C_s^2, \quad \forall (x_0,\xi_0) \in M_b.
\end{aligned}$$

*where $C_s^\ell$, $\ell = 1, 2$ are constants and the sets $M_a = M_a(t)$ and $M_b = M_b(t)$ are defined by*

$$\begin{aligned}
M_a &= \left\{(x_0,\xi_0) \in D \cap M \middle| x(t';x_0,\xi_0) \in \mathring{X}, \forall t' \in [0,t]\right\}, \\
M_b &= \left\{(x_0,\xi_0) \in D \cap M \middle| \exists t' \in (0,t),\ s.t.\ x(t';x_0,\xi_0) \in \partial X\right\}.
\end{aligned}$$

**Proof:** Lemma 2.3 in [28] gives

$$|\partial^\gamma h_t(x_0,\xi_0)| \le C_s^1 e^{(2s-1)LT} t, \quad \forall (x_0,\xi_0) \in M_a.$$

For $(x_0, \xi_0) \in M_b$, one can easily see that there exists $l > 0$, for any $(x_0', \xi_0') \in D \cap M$ which satisfies

$$\left\|(x_0', \xi_0') - (x_0, \xi_0)\right\| < l,$$

$(x_0', \xi_0') \in M_b$ holds.

Moreover, if we choose $l < \frac{2}{L_1} e^{-L_2 T}$, the stability estimate gives

$$\left\|h_t(x_0', \xi_0') - h_t(x_0, \xi_0)\right\| < 2.$$

This implies $x(t; x_0, \xi_0) = x(t; x_0', \xi_0')$ because boundaries are either $x = 1$ or $x = -1$. Therefore

$$\partial^\gamma x(t; x_0, \xi_0) = 0, \quad \forall (x_0, \xi_0) \in M_b.$$

By taking derivatives of energy conservation identity

$$\frac{1}{2}\xi^2(t; x_0, \xi_0) + V(x(t; x_0, \xi_0)) = \frac{1}{2}\xi_0^2 + V(x_0),$$

one has

$$\frac{1}{2}\partial^\gamma \left(\xi^2(t; x_0, \xi_0)\right) = \begin{cases} 1, & s = 2,\ \gamma = (0,2) \\ V^{(s)}(x_0), & \gamma = (s,0) \\ 0, & \text{otherwise.} \end{cases}$$

Here we will only discuss the case of $s = 2$, while the other situations can be proved similarly by direct calculations.

For $\gamma = (0,2), (1,1)$ and $(2,0)$, we have

$$\begin{aligned} \xi_{\xi_0\xi_0} &= \frac{1}{\xi} - \frac{\xi_0 \xi_{\xi_0}}{\xi^2} = \frac{\xi^2 - \xi_0^2}{\xi^3} = \frac{2(V(x_0) - V(x))}{\xi^3}, \\ \xi_{\xi_0 x_0} &= -\frac{\xi_0 \xi_{x_0}}{\xi^2} = -\frac{\xi_0 V'(x_0)}{\xi^3}, \\ \xi_{x_0 x_0} &= \frac{V''(x_0)}{\xi} - \frac{V'(x_0)\xi_{x_0}}{\xi^2} = \frac{\xi^2 V''(x_0) - V'^2(x_0)}{\xi^3}. \end{aligned}$$

Since $V(x) \in C^\infty(X)$, then $E_{(k)} \le \left|V^{(k)}(x)\right| \le E^{(k)}$ where $E_{(k)}$ and $E^{(k)}$ are constants. Hence

$$\begin{aligned} |\xi_{\xi_0\xi_0}| &\le \frac{4E^{(0)}}{(2\epsilon_0)^{3/2}} = C_{(0,2)}, \\ |\xi_{\xi_0 x_0}| &\le \frac{\sqrt{2(H_{\max} - E_{(0)})}E^{(1)}}{(2\epsilon_0)^{3/2}} = C_{(1,1)}, \\ |\xi_{\xi_0 x_0}| &\le \frac{2(H_{\max} - E_{(0)})E^{(2)} + (E^{(1)})^2}{(2\epsilon_0)^{3/2}} = C_{(2,0)}. \end{aligned}$$

Letting $C_2^2 = C_{(0,2)} + C_{(1,1)} + C_{(2,0)}$ yields

$$|\partial^\gamma h_t(x_0, \xi_0)| \leq C_2^2, \quad \forall (x_0, \xi_0) \in M_b,$$

which proves the theorem. ■

**Theorem 3.4** *Assume the accuracy orders of the local interpolation operators $\mathcal{I}_1$ and $\mathcal{I}_2$ are $\alpha \geq 1$ for functions sufficiently smooth, and the $L^\infty$ norm of linear interpolation on continuous functions is h-independent. We define the numerical error at time t as*

$$\epsilon_t = \max_{(x,\xi)\in D\cap M} \left\| h_t(x,\xi) - \widetilde{h}_t(x,\xi) \right\|,$$

*where $h_t$ is the exact solution and $\widetilde{h}_t$ is the numerical solution given in Section 2. Then for finite time $T > 0$,*

$$\epsilon_T \leq C(\Delta t^2 + h),$$

*where $C > 0$ is constant.*

**Proof:** We denote $y = (x, \xi)$ as a short notation for particles. For the grid point $y$, one has

$$\left\| h_{\Delta t}(y) - \widetilde{h}_{\Delta t}(y) \right\| \leq C_0 \Delta t^2.$$

If $y$ is not a grid point, we define $\mathcal{I}_j$ (resp. $\widetilde{\mathcal{I}}_j$) $j = 1, 2$ as the interpolation operators constructed from $h_{\Delta t}$ (resp. $\widetilde{h}_{\Delta t}$) for boundary and standard particles, then $\widetilde{h}_{\Delta t}(y) = \widetilde{\mathcal{I}}_j(y)$ and

$$\left\| h_{\Delta t}(y) - \widetilde{h}_{\Delta t}(y) \right\| \leq$$
$$\begin{cases} \left\| \mathcal{I}_1(y) - \widetilde{\mathcal{I}}_1(y) \right\| + \left\| \mathcal{I}_1(y) - h_{\Delta t}(y) \right\|, & \text{for boundary particles,} \\ \left\| \mathcal{I}_2(y) - \widetilde{\mathcal{I}}_2(y) \right\| + \left\| \mathcal{I}_2(y) - h_{\Delta t}(y) \right\|, & \text{for standard particles,} \\ \left\| \Theta_{\Delta t}(y) - h_{\Delta t}(y) \right\|, & \text{for special partiles.} \end{cases}$$

Denote $N_1$ and $N_2$ to be the h-independent norms of the interpolation operators $\mathcal{I}_1$ and $\mathcal{I}_2$, then

$$\begin{aligned} \left\| \mathcal{I}_1(y) - \widetilde{\mathcal{I}}_1(y) \right\| &\leq N_1 \max_{y\in\{\text{grid points}\}} \left\| h_{\Delta t}(y) - \widetilde{h}_{\Delta t}(y) \right\| \leq C_0 N_1 \Delta t^2, \\ \left\| \mathcal{I}_2(y) - \widetilde{\mathcal{I}}_2(y) \right\| &\leq N_2 \max_{y\in\{\text{grid points}\}} \left\| h_{\Delta t}(y) - \widetilde{h}_{\Delta t}(y) \right\| \leq C_0 N_2 \Delta t^2. \end{aligned}$$

Since $\mathcal{I}_1$ and $\mathcal{I}_2$ are smooth interpolations, they have Lipschitz constants $L_{\mathcal{I}_1}$ and $L_{\mathcal{I}_2}$. As $y$ is not a grid point, we can find a grid point $y_1$ such that

$$\|y - y_1\| \leq h,$$

then

$$\begin{aligned}
& \|\mathcal{I}_1(y) - h_{\Delta t}(y)\| \\
\leq\ & \|\mathcal{I}_1(y) - \mathcal{I}_1(y_1)\| + \|\mathcal{I}_1(y_1) - h_{\Delta t}(y_1)\| + \|h_{\Delta t}(y_1) - h_{\Delta t}(y)\| \\
\leq\ & L_{\mathcal{I}_1} \|y - y_1\| + C_1 h^\alpha \max_{|\gamma|=\alpha} \sup_{y_0 \in M_b} \|\partial^\gamma h_{\Delta t}(y_0)\| + L_1 e^{L_2 \Delta t} \|y - y_1\| \\
\leq\ & C_2 h + C_3 h^\alpha,
\end{aligned}$$

and

$$\begin{aligned}
& \|\mathcal{I}_2(y) - h_{\Delta t}(y)\| \\
\leq\ & \|\mathcal{I}_2(y) - \mathcal{I}_2(y_1)\| + \|\mathcal{I}_2(y_1) - h_{\Delta t}(y_1)\| + \|h_{\Delta t}(y_1) - h_{\Delta t}(y)\| \\
\leq\ & L_{\mathcal{I}_2} \|y - y_1\| + C_4 h^\alpha \max_{|\gamma|=\alpha} \sup_{y_0 \in M_b} \|\partial^\gamma h_{\Delta t}(y_0)\| + L_1 e^{L_2 \Delta t} \|y - y_1\| \\
\leq\ & C_5 h + C_6 h^\alpha \Delta t.
\end{aligned}$$

Therefore the error term $\epsilon_{\Delta t}$ satisfies

$$\epsilon_{\Delta t} \leq C_7 \Delta t^2 + C_8 h + C_9 h^\alpha + C_{10} h^\alpha \Delta t.$$

For a grid point $y$, we can further derive

$$\begin{aligned}
& \left\| h_{2\Delta t}(y) - \widetilde{h}_{2\Delta t}(y) \right\| \\
\leq\ & \left\| h_{\Delta t}(h_{\Delta t}(y)) - h_{\Delta t}(\widetilde{h}_{\Delta t}(y)) \right\| + \left\| h_{\Delta t}(\widetilde{h}_{\Delta t}(y)) - \widetilde{h}_{\Delta t}(\widetilde{h}_{\Delta t}(y)) \right\| \\
\leq\ & L_1 e^{L_2 \Delta t} \epsilon_{\Delta t} + \epsilon_{\Delta t} = L_3 \frac{e^{2L_2 \Delta t} - 1}{e^{L_2 \Delta t} - 1} \epsilon_{\Delta t},
\end{aligned}$$

and

$$\epsilon_{B\Delta t} = \left\| h_{B\Delta t}(y) - \widetilde{h}_{B\Delta t}(y) \right\| \leq L_3^B \frac{e^{L_2 B \Delta t} - 1}{e^{L_2 \Delta t} - 1} \epsilon_{\Delta t},$$

where

$$L_3 = \max(L_1, 1).$$

If $y$ is not a grid point, similarly we have

$$\begin{aligned}
\epsilon_{B\Delta t} &\leq (N_1 + N_2) L_3^B \cdot \frac{e^{L_2 B \Delta t} - 1}{e^{L_2 \Delta t} - 1} \epsilon_{\Delta t} + \epsilon_{\Delta t} + C_{10} h^\alpha B \Delta t \\
&\leq (N_1 + N_2 + 1) L_3^B \cdot \frac{e^{L_2 B \Delta t} - 1}{e^{L_2 \Delta t} - 1} \epsilon_{\Delta t} + C_{10} h^\alpha B \Delta t \\
&= N \cdot \frac{e^{L_2 B \Delta t} - 1}{e^{L_2 \Delta t} - 1} \epsilon_{\Delta t} + C_{10} h^\alpha B \Delta t.
\end{aligned}$$

The recurrence shows that

$$\begin{aligned}
\epsilon_{B^K\Delta t} &\leq N\cdot\frac{e^{L_2B^K\Delta t}-1}{e^{L_2B^{K-1}\Delta t}-1}\epsilon_{B^{K-1}\Delta t}+C_{10}h^\alpha B^K\Delta t\\
&\leq N^K\frac{e^{L_2B^K\Delta t}-1}{e^{L_2\Delta t}-1}\epsilon_{\Delta t}+C_{10}h^\alpha\sum_{k=0}^{K}N^k\frac{e^{L_2B^K\Delta t}-1}{e^{L_2B^{K-k}\Delta t}-1}B^{K-k}\Delta t\\
&\leq N^K\frac{e^{L_2T}-1}{L_2}\epsilon_{\Delta t}+C_{10}h^\alpha\frac{e^{LT}-1}{L}\sum_{k=0}^{K}N^k.
\end{aligned}$$

Hence we have

$$\epsilon_T\leq C(\Delta t^2+h).\blacksquare$$

By (12), Theorem 3.4 implies the convergence result for the solution to Liouville equation (1).

**Theorem 3.5** *Assume initial condition $f_0$ and boundary condition $g$ in* (7)-(8) *are smooth, and $g(t,x,\xi)$ is consistent with $f_0(x,\xi)$ at $t=0$. Define $f(t,x,\xi)$ and $\tilde{f}(t,x,\xi)$ are the solutions* (12) *to Liouville equation* (1) *given by $h_t$ and $\widetilde{h}_t$ separately, then for finite time $T>0$,*

$$\max_{(x,\xi)\in D\cap M}\left\|f(T,x,\xi)-\tilde{f}(T,x,\xi)\right\|\leq\tilde{C}(\Delta t^2+h),$$

*where $\tilde{C}>0$ is constant.*

**Remark 3.6** *Sometimes the coefficients of the linear $h$ terms in the error estimate are much smaller than those of the higher order $h$ terms. This makes the algorithm have higher order convergence rate, as observed in Example 2 of Section 4.1.*

# 4 Numerical examples and Applications

In this section we mainly study the examples appearing in classical mechanics where

$$H=\frac{1}{2}\left|\boldsymbol{\xi}\right|^2+V(\boldsymbol{x}).\tag{22}$$

In the following examples, we compare the $l^1$ errors at time $t=T$ for $h_t$ and $f$. The ratio of averaged number of special particles per iteration(NSP) over the number of total particles(NTP) are also presented in order to study the complexity of the algorithm. We use a second order symplectic solver $\Gamma_{\Delta t}$ presented in [6, 16]. For the interpolation operators $\mathcal{I}_1$, $\mathcal{I}_2$, we use the second order Lagrange polynomial interpolation [20].

### 4.1 Numerical examples

**Example 1.** Consider the 1D Liouville equation

$$f_t + \xi f_x - V_x f_\xi = 0,$$

on the computational domain

$$M = \left\{ (x,\xi) \in [0,1] \times [-0.8, 0.8] \;\middle|\; 0.02 \le H = V(x) + \frac{1}{2}\xi^2 \le 0.18 \right\}.$$

The potential $V(x)$ is given by

$$V(x) = \begin{cases} -0.4(x-0.5)(x+0.5), & 0 \le x < 0.5, \\ 0, & 0.5 \le x \le 1. \end{cases}$$

The initial data is

$$f(x,\xi,0) = 0,$$

and the boundary conditions are

$$\begin{aligned} f(t,1,\xi) &= \begin{cases} -25(\xi+0.2)(\xi+0.6)\sin(2\pi t) & -0.6 \le \xi \le -0.2, \\ 0 & \text{otherwise}, \end{cases} \\ f(t,0,\xi)|_{\xi>0} &= f(t,0,-\xi). \end{aligned}$$

This example has inflow boundary condition at $x = 1$ and reflection boundary condition condition at $x = 0$.

The solution at time $T = 3$ is given in Figure 2. The exact solution is computed by solving the Hamiltonian system analytically. We present the $l^1$ error in Table 1, where the numerical solutions converges at first order. In Table 2, the ratio of NSP over NTP with different mesh are shown. One can observe that the ratio is reduced linearly with the mesh size.

Table 1: the $l^1$ errors for different mesh sizes for Example 1

| mesh | $50 \times 50$ | $100 \times 100$ | $200 \times 200$ | $400 \times 400$ |
|---|---|---|---|---|
| $h_T(x,\xi)$ | $2.46 \times 10^{-3}$ | $1.26 \times 10^{-3}$ | $6.33 \times 10^{-4}$ | $3.18 \times 10^{-4}$ |
| $f(T,x,\xi)$ | $3.11 \times 10^{-3}$ | $1.69 \times 10^{-3}$ | $9.18 \times 10^{-4}$ | $4.79 \times 10^{-4}$ |

**Example 2.** Consider the 1D Liouville equation on the computational domain

$$M = \left\{ (x,\xi) \in [-1,1] \times [-0.8, 0.8] \;\middle|\; 0.02 \le H = V(x) + \frac{1}{2}\xi^2 \le 0.18 \right\},$$

Table 2: NSP versus NTP in Example 1

| mesh | $50 \times 50$ | $100 \times 100$ | $200 \times 200$ | $400 \times 400$ |
|---|---|---|---|---|
| NSP | 147 | 299 | 602 | 1212 |
| NTP | 1372 | 5364 | 21454 | 85826 |
| ratio | 10.71% | 5.57% | 2.81% | 1.41% |

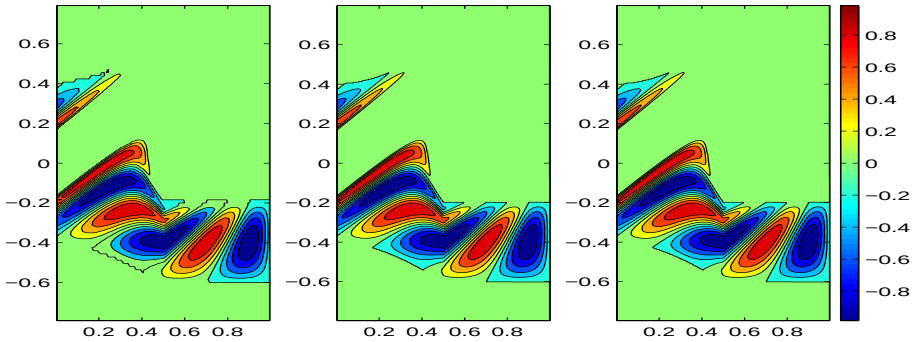


Figure 2: Example 1, phase space solution $f(t, x, \xi)$ at time $t = 3$. From left to right are the numerical solutions using $100 \times 100$ mesh, $400 \times 400$ mesh and the exact solution.

and the potential is given by (see Figure 3)

$$V(x) = \begin{cases} 0.1(4x^2 - 1)^3, & -0.5 \le x \le 0.5, \\ 0, & \text{otherwise.} \end{cases}$$

The initial data is

$$f(x, \xi, 0) = 0,$$

and the boundary conditions are

$$f(t, 1, \xi) = \begin{cases} -25(\xi + 0.2)(\xi + 0.6)\sin(2\pi t) & -0.6 \le \xi \le -0.2, \\ 0 & \text{otherwise,} \end{cases}$$

$$f(t, -1, \xi) = \begin{cases} -25(\xi - 0.2)(\xi - 0.6)\sin(2\pi t) & 0.2 \le \xi \le 0.6, \\ 0 & \text{otherwise.} \end{cases}$$

This is an inflow boundary condition example. The solution at time $T = 2.5$ is given in Figure 4. The 'exact' solution is obtained by numerically solving the Hamiltonian system on a very fine mesh with a very small time step. We present the $l^1$ error and its convergence rate in Table 3. The numerical error is much small than in Example 1. The convergence rate is near second order, which is better than the error estimate given in Section 3.2. In Table 4, we show the ratios of NSP over NTP with different meshes.

Table 3: the $l^1$ errors for different mesh sizes for Example 2

| mesh | $50 \times 50$ | $100 \times 100$ | $200 \times 200$ | $400 \times 400$ |
|---|---|---|---|---|
| $h_T(x, \xi)$ | $9.82 \times 10^{-4}$ | $3.01 \times 10^{-4}$ | $8.66 \times 10^{-5}$ | $2.39 \times 10^{-5}$ |
| convergence rate | $- - -$ | 1.7060 | 1.7973 | 1.8574 |
| $f(T, x, \xi)$ | $1.83 \times 10^{-3}$ | $5.53 \times 10^{-4}$ | $1.55 \times 10^{-4}$ | $4.23 \times 10^{-5}$ |
| convergence rate | $- - -$ | 1.7265 | 1.8350 | 1.8667 |

Table 4: NSP versus NTP in Example 2

| mesh | $50 \times 50$ | $100 \times 100$ | $200 \times 200$ | $400 \times 400$ |
|---|---|---|---|---|
| NSP | 174 | 360 | 711 | 1440 |
| NTP | 1152 | 4532 | 18064 | 72292 |
| ratio | 15.10% | 7.94% | 3.94% | 1.99% |

### 4.2 Applications

In this subsection we study the applications in computation of multivalued solutions to quasilinear PDEs. These problems arise in the semiclassical limit of linear Schrödinger equation, in which the initial condition for (1) and (22) often has the following form

$$f(0, \boldsymbol{x}, \boldsymbol{\xi}) = \rho_0(\boldsymbol{x})\delta(\boldsymbol{\xi} - \boldsymbol{u}_0(\boldsymbol{x})), \tag{23}$$

see for example [5, 17]. In most cases, we are interested in computing the multivalued physical observables, which can be constructed from the moments of $f$,

$$\begin{aligned} \rho(t, \boldsymbol{x}) &= \int f(t, \boldsymbol{x}, \boldsymbol{\xi}) \mathrm{d}\boldsymbol{\xi}, \\ \rho(t, \boldsymbol{x})\boldsymbol{u}(t, \boldsymbol{x}) &= \int \boldsymbol{\xi} f(t, \boldsymbol{x}, \boldsymbol{\xi}) \mathrm{d}\boldsymbol{\xi}. \end{aligned}$$

The initial data (23) is singular, which can destroy numerical accuracy. In [9], a decomposition technique was introduced to solve the multivalued physical observables for smooth potentials. This idea was extended for discontinuous potentials in [12]. See also [25, 26] for discussions of related delta function integrals. Below we will apply this new developed hybrid phase flow method for efficiently computing Liouville equation and constructing multivalued physical observables.

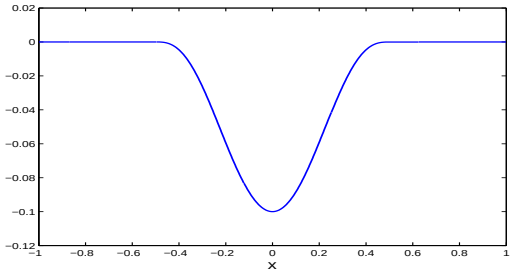


Figure 3: Example 2, potential $V(x)$.

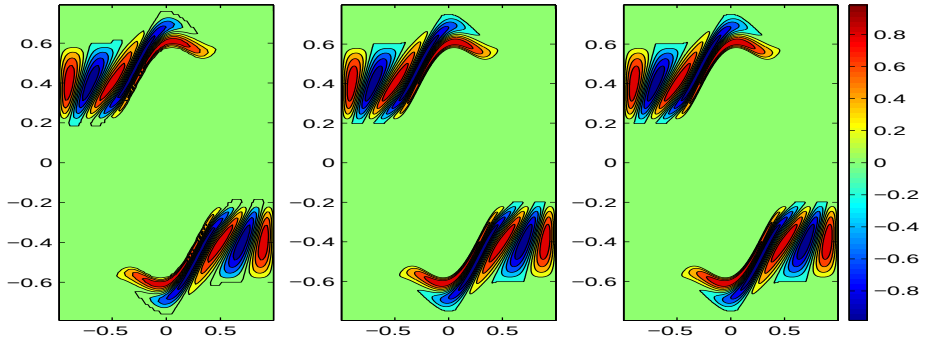


Figure 4: Example 2, phase space solution $f(t, x, \xi)$ at time $t = 2.5$. From left to right are the numerical solutions using $100 \times 100$ mesh, $400 \times 400$ mesh and the exact solution.

**Example 3.** Consider the 1D Liouville equation on the computational domain

$$M = \left\{ (x, \xi) \in [-2, 2] \times [-1.6, 1.6] \,\middle|\, 0 \le H = V(x) + \frac{1}{2}\xi^2 \le 0.65 \right\},$$

with the discontinuous potential given by

$$V(x) = \begin{cases} 0.2, & x < 0, \\ 0, & x > 0. \end{cases}$$

The initial data is

$$f(0, x, \xi) = \begin{cases} \delta(\xi - 0.9 + \frac{0.9}{4}(x+2)^2), & -2 \le x \le 0, \\ \delta(\xi + 0.9 - \frac{0.9}{4}(x-2)^2), & 0 < x \le 2, \end{cases}$$

and the Dirichlet boundary conditions are

$$\begin{aligned} f(t, 2, \xi) &= \delta(\xi + 0.9), \\ f(t, -2, \xi) &= \delta(\xi - 0.9). \end{aligned}$$

This example was first proposed in [12], and the analytical velocity and density functions can be found in its Appendix. We output the numerical solutions of the density $\rho(t,x)$ and velocity $u(t,x)$ with different meshes against the exact solution at time $T = 1.8$ in Figure 5. In Table 5-6, we give the $l^1$ errors of the numerical solutions and the ratios of NSP over NTP. The convergence rate is nearly first order, which agrees with the discussion for interface problem in [13]. This is more accurate than the results in [12], where only halfth order was obtained [27].

Table 5: the $l^1$ errors for different mesh sizes for Example 3

| mesh | $100 \times 100$ | $200 \times 200$ | $400 \times 400$ | $800 \times 800$ |
|---|---|---|---|---|
| $\rho(t,x)$ | $5.01 \times 10^{-1}$ | $2.90 \times 10^{-1}$ | $1.63 \times 10^{-1}$ | $7.77 \times 10^{-2}$ |
| $u(t,x)$ | $4.82 \times 10^{-2}$ | $2.54 \times 10^{-2}$ | $1.44 \times 10^{-2}$ | $5.60 \times 10^{-3}$ |

Table 6: NSP versus NTP in Example 3

| mesh | $100 \times 100$ | $200 \times 200$ | $400 \times 400$ | $800 \times 800$ |
|---|---|---|---|---|
| NSP | 327 | 671 | 1394 | 2858 |
| NTP | 6600 | 26000 | 104800 | 417600 |
| ratio | 4.95% | 2.58% | 1.33% | 0.68% |

**Example 4.** Consider the 2D Liouville equation

$$f_t + \xi f_x + \eta f_y - V_x f_\xi - V_y f_\eta = 0,$$

on the computational domain

$$M = \left\{ (x,y,\xi,\eta) \in [-0.15, 0.21]^2 \times [0.2, 0.5]^2 \;\middle|\; 0.1 \le H(x,y,\xi,\eta) \le 0.26 \right\},$$

with the Hamiltonian

$$H(x,y,\xi,\eta) = V(x,y) + \frac{1}{2}(\xi^2 + \eta^2),$$

and the discontinuous potential given by

$$V(x,y) = \begin{cases} 0, & x+y > 0.11, \\ 0.1, & x+y < 0.11. \end{cases}$$

The initial data is taken as

$$f(0,x,y,\xi,\eta) = \begin{cases} \delta(\xi - 0.2828)\delta(\eta - 0.2828), & -0.1 < x \pm y < 0.1, \\ 0, & \text{otherwise.} \end{cases}$$

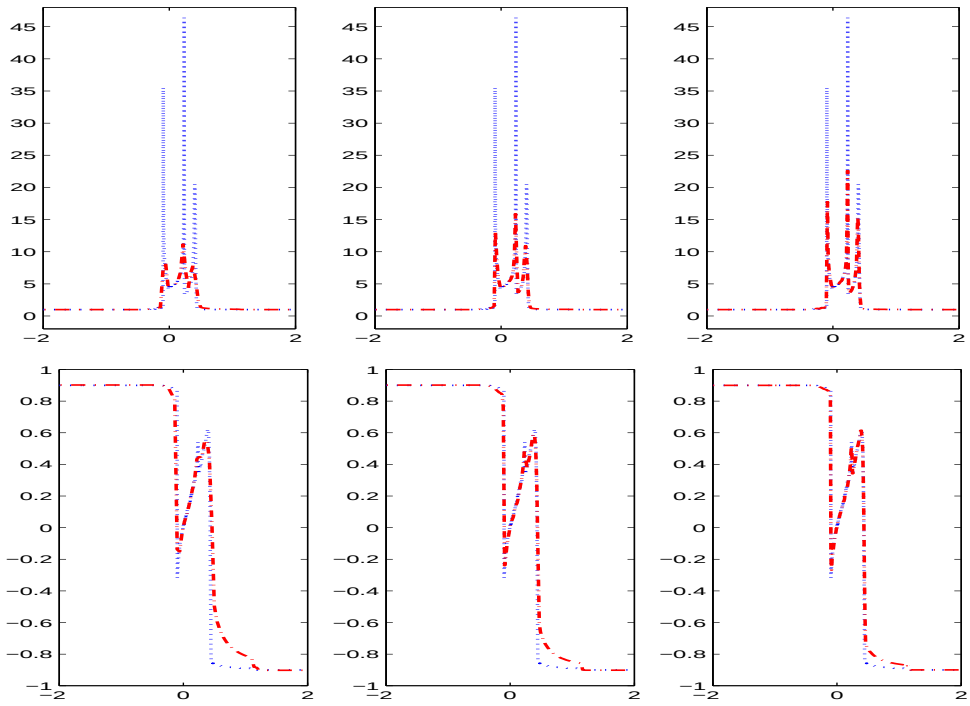

Figure 5: Example 3, density $\rho(t,x)$ (UP) and velocity $u(t,x)$ (DOWN) at time $t = 1.8$. The blue dotted lines are exact solutions and the red dashdot lines are numerical solutions. From left to right are the numerical solution using $100 \times 100$, $200 \times 200$ and $400 \times 400$ mesh.

and the boundary conditions are

$$\begin{aligned} f(t,x,y,\xi,\eta)\big|_{(x,y)\in\partial M,\ (\xi,\eta)\cdot\vec{\boldsymbol{n}}<0} &= 0, \\ \frac{\partial f}{\partial \vec{\boldsymbol{n}}}(t,x,y,\xi,\eta)\big|_{(x,y)\in\partial M,\ (\xi,\eta)\cdot\vec{\boldsymbol{n}}>0} &= 0. \end{aligned}$$

At time $T = 0.1886$, the exact density is

$$\rho(0.1886,x,y) = \begin{cases} \frac{2}{3}, & 0.11 < x+y < 0.255,\ -0.1 < x-y < 0.1, \\ 1, & 0.0067 < x+y < 0.11,\ -0.1 < x-y < 0.1, \\ 0, & \text{otherwise.} \end{cases}$$

We output numerical solutions of the density $\rho(t,x,y)$ with different meshes compared to the exact density in Figure 6. In Table 7-8, we give the $l^1$ errors of numerical solutions and the ratios of NSP over NTP, which imply the same conclusion made in the end of last example.

Table 7: the $l^1$ errors for different mesh sizes for Example 4

| mesh | $26^2 \times 26^2$ | $52^2 \times 52^2$ | $104^2 \times 104^2$ |
|---|---|---|---|
| $\rho(t,x,y)$ | $5.36 \times 10^{-3}$ | $2.49 \times 10^{-3}$ | $1.25 \times 10^{-3}$ |

Table 8: NSP versus NTP in Example 4

| mesh | $26^2 \times 26^2$ | $52^2 \times 52^2$ | $104^2 \times 104^2$ |
|---|---|---|---|
| NSP | 53972 | 453690 | 3263199 |
| NTP | 226305 | 3680948 | 58532127 |
| ratio | 23.85% | 12.33% | 5.58% |

# 5 Conclusion

In this paper, we propose a hybrid phase flow method for solving Liouville equation in bounded domain where the traditional phase flow method has difficulties when the domain size is smaller than the invariant manifold of flow map. This hybrid phase flow method can also help reduce the numerical difficulty when the invariant manifold of phase flow given by Liouville equation is unbounded. The stability and convergence of this method is analyzed and several numerical examples and applications are presented to verify the accuracy and efficiency.

# Acknowledgement

The authors thank Prof. Shi Jin for his valuable discussions.

# References

[1] J. D. Benamou, *Direct computation of multivalued phase space solutions for Hamilton-Jacobi equations*, Comm. Pure Appl. Math. **52** (1999), pp. 1443-1457.

[2] L.T. Cheng, H.L. Liu and S. Osher, *Computational high-frequency wave propagation using the level set method, with applications to the semi-classical limit of Schrödinger equations*, Commun. Math. Sci. **1** (2003), pp. 593-621.

[3] B. Engquist and O. Runborg, *Computational high frequency wave propagation*, Acta Numerica **12** (2003), pp. 181-266.

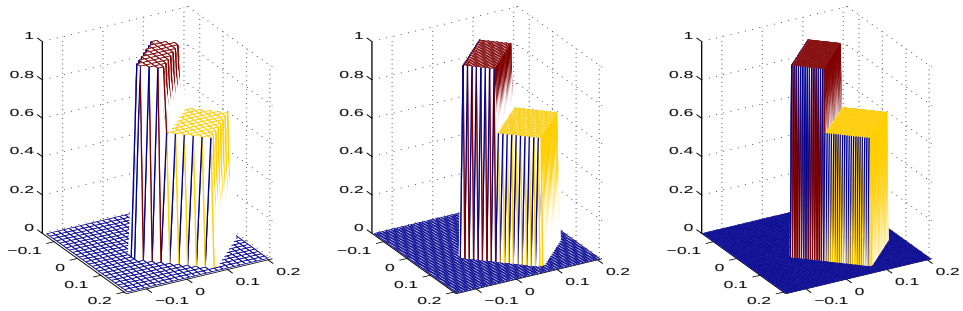

Figure 6: Example 4, density $\rho(t, x, y)$ at time $t = 0.1886$. From left to right are the numerical solutions using $26^2 \times 26^2$ mesh, $52^2 \times 52^2$ mesh and the exact solution.


[4] B. Engquist, O. Runborg and A. K. Tornberg, *High frequency wave propagation by the segment projection method*, J. Comput. Phys. **178** (2002), pp. 373-390.

[5] P. Gérard, P.A. Markowich, N.J. Mauser and F. Poupaud, *Homogenization limits and Wigner transforms*, Comm. Pure Appl. Math. **50** (1997), pp. 321-377.

[6] E. Hairer, C. Lubich and G. Wanner, *Geometric Numerical Integration: Structure-preserving Algorithms for Ordinary Differential Equations*, Springer-Verlag, Berlin, 2002.

[7] S. Jin, *Recent computational methods for high frequency waves in heterogeneous media*, Industrial and Applied Mathematics in China, 49–64, Ser. Contemp. Appl. Math. CAM **10** (2009), Higher Ed. Press, Beijing.

[8] S. Jin and X.T. Li, *Multi-phase computations of the semiclassical limit of the Schrödinger equation and related problems: Whitham vs. Wigner*, Physica D **182** (2003), pp. 46-85.

[9] S. Jin, H.L. Liu, S. Osher and R. Tsai, *Computing multivalued physical observables for the semiclassical limit of the Schrödinger equation*, J. Comput. Phys. **205** (2005), pp. 222-241.

[10] S. Jin and K. Novak, *A Semiclassical Transport Model for Two-dimensional Thin Quantum Barriers*, J. Comput. Phys. **226** (2007), pp. 1623-1644.

[11] S. Jin and S. Osher, *A level set method for the computation of multivalued solutions to quasi-linear hyperbolic PDEs and Hamilton-Jacobi Equations*, Commun. Math. Sci. **1** (2003), pp. 575-591.

[12] S. Jin and X. Wen, *Hamiltonian-preserving schemes for the Liouville equation of discontinuous potential*, Commun. Math. Sci. **3** (2005), pp. 285-315.

[13] S. Jin, H. Wu and Z.Y. Huang, *A Hybrid Phase-Flow Method for Hamiltonian Systems with Discontinuous Hamiltonians*, SIAM J. Sci. Comput. **31** (2008), pp. 1303-1321.

[14] S. Jin, H. Wu and X. Yang, *Gaussian beam methods for the Schrodinger equation in the semi-classical regime: Lagrangian and Eulerian formulations*, Commun. Math. Sci. **6** (2008), no. 4, pp. 995-1020.

[15] J.B. Keller and R.M. Lewis, *Asymptotic methods for partial differential equations: the reduced wave equation and Maxwell's equations*, Surveys in applied mathematics **1** (1995), pp. 1-82.

[16] B. Leimkuhler and S. Reich, *Simulating Hamiltonian Dynamics*, Cambridge University Press, 2004.

[17] P.L. Lions and T. Paul, *Sur les measures de Wigner*, Revista Matemática Iberoamericana **9** (1993), pp. 553-618.

[18] G. Papanicolaou and L. Ryzhik, *Waves and Transport*, IAS/Park City Math. Series **5**, 305-382, 1998, L. Caffarelli and Weinan E eds.

[19] M. M. Popov, *A new method of computation of wave fields using gaussian beams*, Wave Motion **4** (1982), pp. 85-97.

[20] K. Rainer, *Numerical Analysis*, Springer, New York, 1998.

[21] J. Ralston, *Gaussian beams and the propagation of singularities*, Studies in PDEs, MAA stud. Math. **23** (1982), pp. 206-248.

[22] O. Runborg, *Mathematical models and numerical methods for high frequency waves*, Commun. Comput. Phys. **2** (2007), no. 5, pp. 827–880.

[23] C. Sparber, P.A. Markowich and N.J. Mauser, *Wigner functions versus WKB-methods in multivalued geometrical optics*, Asymptotic Analysis **33** (2003), pp. 153-187.

[24] N. M. Tanushev, *Superpositions and higher order Gaussian beams*, Commun. Math. Sci. **6** (2008), no. 2, pp. 449-475.

[25] X. Wen, *High order numerical methods to a type of delta function integrals*, J. Comput. Phys. **226** (2007), pp. 1952-1967.

[26] X. Wen, *High order numerical quadratures to one dimensional delta function integrals*, SIAM J. Sci. Comput. **30** (2008), 1825-1846. .

[27] X. Wen and S. Jin, *The $l^1$-error estimates for a Hamiltonian-preserving scheme to the Liouville equation with piecewise constant coefficients*, J. Comput. Math., to appear.

[28] L.X. Ying and E.J. Candés, *The Phase flow method*, J. Comput. Phys. **220** (2006), pp. 184-215.